

This is a repository copy of *Transient enhancement of magnetization damping in CoFeB film via pulsed laser excitation*.

White Rose Research Online URL for this paper:

<https://eprints.whiterose.ac.uk/116692/>

Version: Published Version

Article:

Liu, Bo, Ruan, Xuezhong, Wu, Zhenyao et al. (7 more authors) (2016) Transient enhancement of magnetization damping in CoFeB film via pulsed laser excitation. *Applied Physics Letters*. 042401. ISSN 0003-6951

<https://doi.org/10.1063/1.4959266>

Reuse

Items deposited in White Rose Research Online are protected by copyright, with all rights reserved unless indicated otherwise. They may be downloaded and/or printed for private study, or other acts as permitted by national copyright laws. The publisher or other rights holders may allow further reproduction and re-use of the full text version. This is indicated by the licence information on the White Rose Research Online record for the item.

Takedown

If you consider content in White Rose Research Online to be in breach of UK law, please notify us by emailing eprints@whiterose.ac.uk including the URL of the record and the reason for the withdrawal request.

Transient enhancement of magnetization damping in CoFeB film via pulsed laser excitation

Bo Liu, Xuezhong Ruan^{*}, Zhenyao Wu, Hongqing Tu, Jun Du, Jing Wu, Xianyang Lu, Liang He, Rong Zhang, and Yongbing Xu^{*}

Citation: *Appl. Phys. Lett.* **109**, 042401 (2016); doi: 10.1063/1.4959266

View online: <http://dx.doi.org/10.1063/1.4959266>

View Table of Contents: <http://aip.scitation.org/toc/apl/109/4>

Published by the [American Institute of Physics](#)



**FIND THE NEEDLE IN THE
HIRING HAYSTACK**

POST JOBS AND REACH THOUSANDS OF
QUALIFIED SCIENTISTS EACH MONTH.

PHYSICS TODAY | JOBS
WWW.PHYSICSTODAY.ORG/JOBS

Transient enhancement of magnetization damping in CoFeB film via pulsed laser excitation

Bo Liu,¹ Xuezhong Ruan,^{1,a)} Zhenyao Wu,¹ Hongqing Tu,² Jun Du,² Jing Wu,³ Xianyang Lu,³ Liang He,¹ Rong Zhang,¹ and Yongbing Xu^{1,3,a)}

¹Jiangsu Provincial Key Laboratory of Advanced Photonic and Electronic Materials, Jiangsu Provincial Key Laboratory for Nanotechnology, Collaborative Innovation Center of Advanced Microstructures, School of Electronic Science and Engineering, Nanjing University, Nanjing 210093, People's Republic of China

²Department of Physics, Nanjing University, Nanjing 210093, People's Republic of China

³York-Nanjing International Joint Center in Spintronics, Departments of Electronics and Physics, The University of York, York YO10 5DD, United Kingdom

(Received 16 April 2016; accepted 2 July 2016; published online 25 July 2016)

Laser-induced spin dynamics of in-plane magnetized CoFeB films has been studied by using time-resolved magneto-optical Kerr effect measurements. While the effective demagnetization field shows little dependence on the pump laser fluence, the intrinsic damping constant has been found to be increased from 0.008 to 0.076 with the increase in the pump fluence from 2 mJ/cm² to 20 mJ/cm². This sharp enhancement has been shown to be transient and ascribed to the heating effect induced by the pump laser excitation, as the damping constant is almost unchanged when the pump-probe measurements are performed at a fixed pump fluence of 5 mJ/cm² after irradiation by high power pump pulses. *Published by AIP Publishing.* [<http://dx.doi.org/10.1063/1.4959266>]

The magnetic tunnel junction (MTJ) structures have been widely investigated for the applications of next generation magnetic storage devices due to their high magnetoresistance (MR) ratio.¹ Among these MTJ structures, the MR values of CoFeB films with MgO barriers are especially high, which have been reported by many groups.^{2,3} In recent years, for a step further in the application of magnetic random access memory (MRAM), the spin transfer torque MRAM (STT-MRAM) utilizing MTJs has also been reported.^{4–6} To reduce the critical current of the writing process in the STT-MRAM, the magnetic materials should have low damping constants. However, high damping constants are favorable to reduce the spin switching time, and thus increase the operating speed. Therefore, besides enhancing the anisotropy constant and MR ratio, it is of great importance to study the mechanism of affecting the damping constant.

To fully understand the underlying physics for the Gilbert damping constant, many works have been done.^{7–10} The increase in damping values can be caused by several possible mechanisms. It is reported that Gilbert damping intrinsically originates from the spin orbital interaction and is proportional to ξ^2/W , where ξ is the spin orbital coupling energy and W is the d -band width.^{11,12} In addition, some other factors, such as thickness, capping layer, and magnetic anisotropy, affect the damping constant as well.^{10,13,14} When the thickness of ferromagnetic (FM) layers is sufficiently thin, the spin current generated by the FM layer will flow into the adjacent layer, which increases the electron scattering rate and thus enhances the damping values. In recent years, a powerful pump-probe technique (the time-resolved magneto-optical Kerr effect, TRMOKE) is employed to obtain the damping constant, which is to some extent equal to the conventional ferromagnetic resonance (FMR). However,

compared with the FMR method, the choice of the fluence of the pump pulses is a key factor when performing the TRMOKE measurements. Generally, low pump fluence is used to avoid the nonlinear excitation and sample surface damage. But when the sample is irradiated in a rational pump fluence range, it is an open question of how does the pulse laser modulates the dynamics of the magnetization. Several groups^{15–18} have reported the effect of the pump fluence on damping constants and other dynamic parameters such as the precessional frequency and the relaxation time. Both the increase^{15–18} and decrease¹⁵ of damping constants caused by the pump fluence have been reported in these works, but few of them extracted the high field limit values from effective damping constants to exclude the contribution of the magnetic anisotropy. In addition, the mechanism of how the pump fluence affects the damping constants has been not clear so far. Here, we present a systematic work on external magnetic field dependence of the damping constant under different laser excitations using TRMOKE measurements. The extracted damping constants at high field limit are found to increase as the pump fluence goes up. During the measurements, we observed little dependence of the effective demagnetization field $4\pi M_{eff}$ on the pump fluence. We found that the increase in the intrinsic damping constant is related to a transient heat effect induced by the pump laser occurring during the measurements.

The Ta (2 nm)/CoFeB (10 nm) were deposited on the MgO (100) substrate by DC magnetron sputtering with a base pressure of 6×10^{-6} Pa. The 2 nm Ta capping layer was used for protecting the CoFeB layer from oxidation. An in-plane hysteresis loop was depicted in Fig. 1(b), which was measured by a vibrating sample magnetometer (VSM). The coercivity H_C was around 12 Oe and the saturation magnetization M_s is 767 emu/cm³, which were comparable to those published in other papers.^{18–20} Fig. 1(a) shows the geometry diagram of our TRMOKE measurements. The pump beam normally incidents on the sample with a spot size of 500 μ m

^{a)} Authors to whom correspondence should be addressed. Electronic addresses: xzruan@nju.edu.cn and ybxu@nju.edu.cn

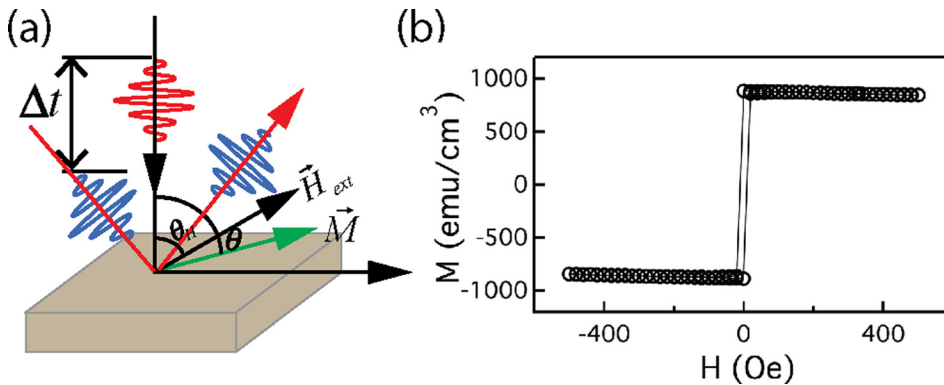


FIG. 1. (a) Schematic of the TRMOKE measurements. (b) Magnetic hysteresis loop for the 10 nm CoFeB film measured by VSM. The external field was applied along the direction of the in-plane easy axis.

in diameter, and the incident angle of probe beam is around 4° away from the normal direction of the film plane with a spot size of $200\ \mu\text{m}$ in diameter. In order to pull the magnetization out of plane, the external magnetic field H is applied at an angle of 60° away from the sample normal direction, labeled as θ_H , and thus the probe laser should be sensitive to the component of magnetization projected on the normal direction of the film plane. The angle θ represents the equilibrium direction of the sample magnetization. This TRMOKE experiment was performed using a pulsed Ti: sapphire regenerative amplifier with a central wavelength of 800 nm, a repetition rate of 1 kHz, and a pulse duration of 60 fs.

Fig. 2(a) shows TRMOKE curves of the 10 nm CoFeB film at different external magnetic fields with the pump fluence $F_p = 10\ \text{mJ}/\text{cm}^2$ and $\theta_H = 60^\circ$. This magnetization dynamics process was initialized by a fs pump pulse laser which modified the anisotropy field at 1–10 ps time scale and thus the magnetization was triggered out of equilibrium, after which the collective spins began to precess around the newly balanced effective field consisting of the magnetic anisotropy field and the external field. The damped oscillations that visualized the dynamics of magnetization relaxation generally lasted for about hundreds of picoseconds. To analyze the data quantitatively, we use a phenomenological formula to fitting these time-resolved Kerr traces

$$\theta_K \propto A \exp(-t/\tau) \sin[2\pi(f + bt)t + \phi_0] + B(t), \quad (1)$$

where A , τ , f , and ϕ_0 are the initial amplitude of the magnetization precession, the relaxation time, the precession frequency, and the initial phase, respectively. The background

term $B(t)$ accounting for the slower demagnetization recovery^{15,21} is generally a summation of one or two exponential functions. The term b in Eq. (1) depicted the tiny frequency shift with time caused by the small pump-induced changes of the magnetic parameters such as M_s and K_U in the probe area. The presence of this extra frequency shift term was also reported in Co_2MnSi Heusler alloy films.²² By fitting the transient Kerr traces in Fig. 2(a) with Eq. (1), we obtained the spin wave precession frequency f (Fig. 2(b)) and the relaxation time τ under different pump fluences. All the data shown in Fig. 2 are obtained under the pump fluence of $F_p = 10\ \text{mJ}/\text{cm}^2$. We also obtained the data under other pump fluences, which exhibited similar trend to those in Fig. 2(a). As shown in Fig. 2(b), the precession frequency f behaves nonlinearly in the low field region, while at high external field, it increases linearly as the field grows up. According to Eqs. (3) and (4), the magnetic anisotropy contribution can be neglected when the external magnetic field is high enough. The red solid line in Fig. 2(b) denotes the calculated values of f , and the formulas are expressed as¹⁷

$$f = (\gamma/2\pi)\sqrt{H_1 H_2}, \quad (2)$$

$$H_1 = H \cos(\theta_H - \theta) - 4\pi M_{\text{eff}} \cos^2 \theta, \quad (3)$$

$$H_2 = H \cos(\theta_H - \theta) - 4\pi M_{\text{eff}} \cos 2\theta. \quad (4)$$

These formulas were derived based on the Landau-Lifshitz-Gilbert (LLG) equation under the linear approximation of uniform precession when taking into account the shape and perpendicular magnetic anisotropy. Here, $4\pi M_{\text{eff}}$ and γ are the effective demagnetization field and the gyromagnetic

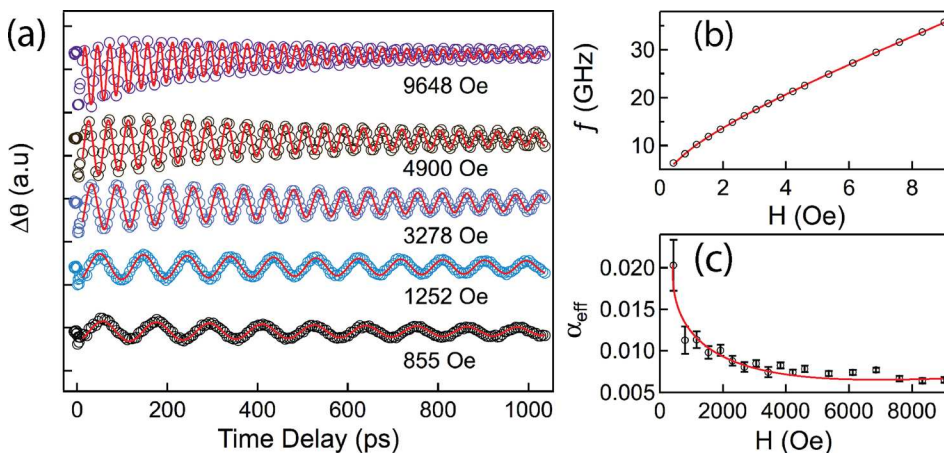


FIG. 2. (a) Typical spin wave dynamic curves (open circles) under different external field with $\theta_H = 60^\circ$ and $F_p = 10\ \text{mJ}/\text{cm}^2$ and their fitting lines (red solid line) according to Eq. (1). (b) The fitted parameter f , the spin wave precession frequency, dependence with external field (open circles). The red solid line represents the fitting line. (c) The magnetic field dependent effective damping values (α_{eff}). The red solid line is a guide to eyes.

ration, respectively. γ is defined as $\gamma \equiv g\mu_B/\hbar$, where g , μ_B , and \hbar are the Lande's g -factor, Bohr magneton, and the Planck's constant, respectively. θ in the above equations is the angle between the equilibrium position of magnetization and the normal direction of the film plane, which is determined from the following equation:

$$\sin 2\theta = (2H/4\pi M_{\text{eff}}) \sin(\theta - \theta_H), \quad (5)$$

where θ_H denoted the angle between the normal direction of the film and external field and was fixed at 60° in all the measurements. Combined with Equations (2)–(5), we obtained the calculated f values (shown in Fig. 2(b)) with the best fitting parameters of $4\pi M_{\text{eff}}$ and g factor. The extracted fitting parameters $4\pi M_{\text{eff}}$ under different pump fluences are plotted in Fig. 3(a) and show no explicit dependence on F_p in this measured excitation range. This indicates that the pump fluences applied in this range have negligible influence on magnetic anisotropy field. The effective damping constants at different external fields are illustrated in Fig. 2(c), in which α_{eff} is given by $\alpha_{\text{eff}} = (2\pi f\tau)^{-1}$. The pump fluence here is 10 mJ/cm^2 . The evolutions of α_{eff} with the applied field under four different pump fluences are similar, which increase sharply with the decrease in the field strength and saturate to constants at high fields. The effective damping constant α_{eff} at high field limit labeled as α_0 extracted from Fig. 2(c) is plotted in Fig. 3(b). Generally, the α_{eff} consists of intrinsic and extrinsic components^{15,23} and the extrinsic part mainly includes the contributions of the magnetic anisotropy field and the multiple-mode excitation spin waves, for example, standing spin waves. The latter occurs usually in thick films²⁴ (for example 20 nm) and should be found at least two frequency modes in the frequency domain. Therefore, in our case, the multiple-mode spin wave contribution should be excluded. In addition, from Fig. 2(c), the strong magnetic field dependence of α_{eff} indicates that the dominant extrinsic contribution should be from magnetic anisotropy field. Since the α_0 contains negligible contribution of the anisotropy field and at the same time $4\pi M_{\text{eff}}$ shows no obvious relationship with F_p , we could infer that the increase

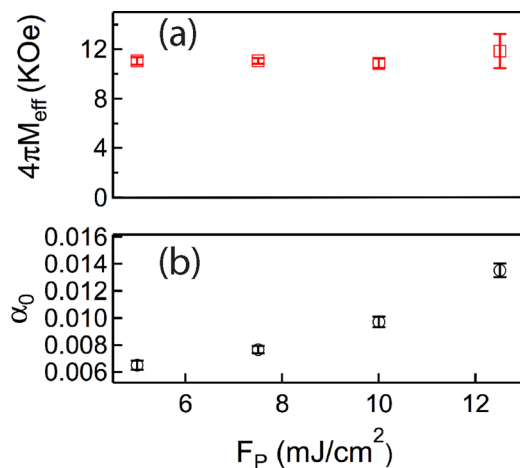


FIG. 3. (a) The extracted effective demagnetization field ($4\pi M_{\text{eff}}$) (red squares) under four different pump excitations. (b) High field limit values α_0 (black squares), which are extracted from the effective damping constants, for different pump fluences.

in α_0 with F_p is not caused by the change in magnetic anisotropy field, which is verified not to be explicitly modified by the pump pulse laser.

To clarify the mechanism that determines the enhancement of α_0 , we compare the α_{eff} measured at increasing pump fluence (black circles in Fig. 4) and those at a fixed pump fluence of $F_p = 5 \text{ mJ/cm}^2$ after irradiated under the increasing F_p for several minutes (red squares in Fig. 4). In Fig. 4, all measurements are performed at $\theta_H = 60^\circ$ and $H = 4900 \text{ Oe}$, where the extracted α_{eff} constants also contain negligible extrinsic contribution. Obviously, the α_{eff} (black circles) constants increase continuously under the increasing pump fluence but remain almost unchanged (red circles) when measured at a fixed low pump power after irradiation under different pump fluences for several minutes. These results demonstrate that the enhancement of α_{eff} is transient and only exists in the presence of high pump fluence but dropped to its original value when the pump laser was set to initialization F_p . This reversible process indicates that the damping constants of the CoFeB sample stay unchanged after being irradiated under high pump fluences. This means that the transient increased damping is not caused by the sample damage or crystallization that may occur at high temperatures. With confirming the validity of the measured damping constants under high pump fluences, one would need to consider if the transient high temperature induced by the pulse heat is the key factor of the transient damping enhancement. According to Carpenne *et al.*,²⁵ we have calculated the maximum electron temperature on the arrival of pulse laser yielding $T_e \sim 1000 \text{ K} - 3000 \text{ K}$ in the range of our pump fluences. Here, we have employed the parameters of the metallic Fe and Co. We believe, however, the electronic response of the CoFeB is similar to that of the metallic Fe and Co. By employing two-temperature model as well the parameters of Fe,²⁶ the spin and lattice temperatures are approximately evaluated to be around $389 \text{ K} - 1100 \text{ K}$ within 10 ps time scale for different pump fluences. Hence, by increasing

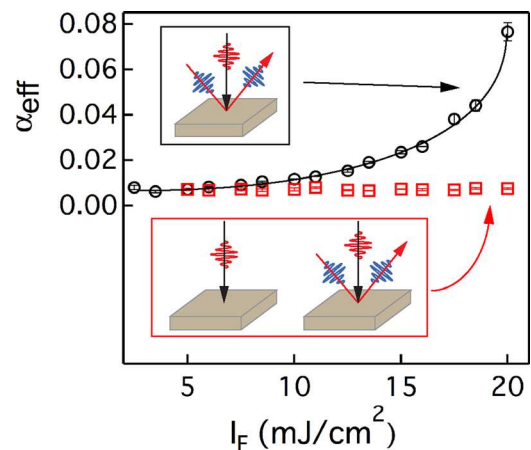


FIG. 4. Pump irradiation fluence (I_F) dependence of effective damping constants extracted at the field of 4900 Oe. The black circles represent the effective damping constants under different pump fluences; whereas, the effective damping constants represented by the red squares were obtained at a fixed pump fluence of 5 mJ/cm^2 , before which the sample was exposed under the indicated illuminations of the laser pulse. The measurement configurations for black circles and red squares are illustrated in the upside and downside of insets, respectively. The solid line is a guide to eyes.

the pump fluence, the ratio of the system temperature T to Curie temperature T_C is increasing. This transient enhancement of damping constant accompanied with the growing ratio is consistent with the theoretical model proposed by Nieves *et al.*²⁷ that the magnetization relaxation time fundamentally depends on susceptibility, which is strongly temperature dependent. Several previous works^{17,18,23,28} have reported the effective damping constant changed with laser fluence, but few of them claimed the change of α_{eff} was permanent or just temporary within the irradiation period. Our work ambiguously confirms that the enhancement of both α_0 and α_{eff} should be a consequence of the increasing ratio of T to T_C caused by the transient heat effect of pump laser.

In conclusion, Gilbert damping constants of the in-plane magnetized Ta/CoFeB (10 nm)/MgO film was studied using the TRMOKE measurements. The effective damping constant α_{eff} of the observed single-frequency magnetization precession was found to decrease with increasing the magnetic field at low field limit, suggesting a contribution of magnetic anisotropy to the enhanced damping at low fields. Both intrinsic α_0 and α_{eff} values were found to increase when applying rational increasing pump fluence, while the effective demagnetization field $4\pi M_{eff}$ showed no obvious pump fluence dependence. Combined with two-temperature model and the theoretical model of Nieves *et al.*, we ascribe this enhancement of the damping constant to the increasing ratio of T/T_C caused by the transient heating effect from the pump laser excitation that does not modify the magnetic anisotropy field. By fixing the F_p of the pump pulse at a low level during the measurements, no enhancement of α_{eff} was observed with the increase in the irradiation fluencies, which demonstrated unambiguously that variation of the damping constants is transient and reversible under a certain pump fluence range. The underlined mechanism of how this heat effect dominates the damping constant calls for detailed experimental and theoretical studies.

This work was supported by the National Basic Research Program of China (No. 2014CB921101), the National Natural Science Foundation of China (Nos. 61274102, 11304148, 21173040, 21373045, 11404056, 21525311, 51471085, and 51331004), and the Natural Science Foundation of Jiangsu Province of China (Nos. BK20130016 and BK2012322).

¹C. Tiusan, M. Sicot, M. Hehn, C. Belouard, S. Andrieu, F. Montaigne, and A. Schuhl, *Appl. Phys. Lett.* **88**, 062512 (2006).

- ²S. S. P. Parkin, C. Kaiser, A. Panchula, P. M. Rice, B. Hughes, M. Samant, and S. H. Yang, *Nat. Mater.* **3**, 862 (2004).
- ³S. Ikeda, J. Hayakawa, Y. Ashizawa, Y. M. Lee, K. Miura, H. Hasegawa, M. Tsunoda, F. Matsukura, and H. Ohno, *Appl. Phys. Lett.* **93**, 082508 (2008).
- ⁴S. Mizukami, E. P. Sajitha, D. Watanabe, F. Wu, T. Miyazaki, H. Naganuma, M. Oogane, and Y. Ando, *Appl. Phys. Lett.* **96**, 152502 (2010).
- ⁵M. Nakayama, T. Kai, N. Shimomura, M. Amano, E. Kitagawa, T. Nagase, M. Yoshikawa, T. Kishi, S. Ikegawa, and H. Yoda, *J. Appl. Phys.* **103**, 07A710 (2008).
- ⁶S. Mangin, D. Ravelosona, J. A. Katine, M. J. Carey, B. D. Terris, and E. E. Fullerton, *Nat. Mater.* **5**, 210 (2006).
- ⁷A. Capua, S.-H. Yang, T. Phung, and S. S. P. Parkin, *Phys. Rev. B* **92**, 224402 (2015).
- ⁸K. Zakeri, J. Lindner, I. Barsukov, R. Meckenstock, M. Farle, U. von Horsten, H. Wende, W. Keune, J. Rucker, S. S. Kalarickal, K. Lenz, W. Kuch, K. Baberschke, and Z. Frait, *Phys. Rev. B* **76**, 104416 (2007).
- ⁹N. Mo, J. Hohlfield, M. ul Islam, C. S. Brown, E. Girt, P. Krivosik, W. Tong, A. Rebei, and C. E. Patton, *Appl. Phys. Lett.* **92**, 022506 (2008).
- ¹⁰A. Natarajaratnam, Z. R. Tadisina, T. Mewes, S. Watts, E. Chen, and S. Gupta, *J. Appl. Phys.* **112**, 053909 (2012).
- ¹¹P. He, X. Ma, J. W. Zhang, H. B. Zhao, G. Lupke, Z. Shi, and S. M. Zhou, *Phys. Rev. Lett.* **110**, 077203 (2013).
- ¹²A. J. Schellekens, L. Deen, D. Wang, J. T. Kohlhepp, H. Swagten, and B. Koopmans, *Appl. Phys. Lett.* **102**, 082405 (2013).
- ¹³Y. Tserkovnyak, A. Brataas, and G. E. W. Bauer, *Phys. Rev. B* **66**, 224403 (2002).
- ¹⁴G. Malinowski, K. C. Kuiper, R. Lavrijsen, H. Swagten, and B. Koopmans, *Appl. Phys. Lett.* **94**, 102501 (2009).
- ¹⁵Z. Chen, M. Yi, M. Chen, S. Li, S. Zhou, and T. Lai, *Appl. Phys. Lett.* **101**, 222402 (2012).
- ¹⁶S. Mizukami, F. Wu, A. Sakuma, J. Walowski, D. Watanabe, T. Kubota, X. Zhang, H. Naganuma, M. Oogane, and Y. Ando, *Phys. Rev. Lett.* **106**, 117201 (2011).
- ¹⁷S. Mizukami, H. Abe, D. Watanabe, M. Oogane, Y. Ando, and T. Miyazaki, *Appl. Phys. Express* **1**, 121301 (2008).
- ¹⁸S. Iihama, Q. L. Ma, T. Kubota, S. Mizukami, Y. Ando, and T. Miyazaki, *Appl. Phys. Express* **5**, 083001 (2012).
- ¹⁹S. Iihama, S. Mizukami, H. Naganuma, M. Oogane, Y. Ando, and T. Miyazaki, *Phys. Rev. B* **89**, 174416 (2014).
- ²⁰T. Liu, Y. Zhang, J. W. Cai, and H. Y. Pan, *Sci. Rep.* **4**, 5895 (2014).
- ²¹S. Mizukami, D. Watanabe, T. Kubota, X. M. Zhang, H. Naganuma, M. Oogane, Y. Ando, and T. Miyazaki, *Appl. Phys. Express* **3**, 123001 (2010).
- ²²Y. Liu, L. R. Sheldford, V. V. Kruglyak, R. J. Hicken, Y. Sakuraba, M. Oogane, and Y. Ando, *Phys. Rev. B* **81**, 094402 (2010).
- ²³S. Mizukami, S. Iihama, N. Inami, T. Hiratsuka, G. Kim, H. Naganuma, M. Oogane, and Y. Ando, *Appl. Phys. Lett.* **98**, 052501 (2011).
- ²⁴J. Walowski, M. D. Kaufmann, B. Lenk, C. Hamann, J. McCord, and M. Münzenberg, *J. Phys. D: Appl. Phys.* **41**, 164016 (2008).
- ²⁵E. Carpene, E. Mancini, C. Dallera, M. Brenna, E. Puppini, and S. De Silvestri, *Phys. Rev. B* **78**, 174422 (2008).
- ²⁶C. Kittel, *Introduction to Solid State Physics* (Wiley, 2005).
- ²⁷P. Nieves, D. Serantes, U. Atxitia, and O. Chubykalo-Fesenko, *Phys. Rev. B* **90**, 104428 (2014).
- ²⁸G. M. Müller, M. Münzenberg, G.-X. Miao, and A. Gupta, *Phys. Rev. B* **77**, 020412 (2008).